Confronting theoretical models with the observed evolution of the galaxy population out to z=4

Bruno Henriques[1]⋆, Simon White[1], Gerard Lemson[1], Peter Thomas[2],
Qi Guo[3,4], Gabriel-Dominique Marleau[1,5], Roderik Overzier[1]

[1]*Max-Planck-Institut für Astrophysik, Karl-Schwarzschild-Str. 1, 85741 Garching b. München, Germany*
[2]*Astronomy Centre, University of Sussex, Falmer, Brighton BN1 9QH, United Kingdom*
[3]*Partner Group of the Max-Planck-Institut für Astrophysik, National Astronomical Observatories, Chinese Academy of Sciences,
  Beijing, 100012, China*
[4]*Department of Physics, Institute for Computational Cosmology, University of Durham, South Road, Durham DH1 3LE*
[5]*Department of Physics, McGill University, 3600 Rue University, Montréal, QC H3A 2T8, Canada*

ABSTRACT

We construct lightcones for the semi-analytic galaxy formation simulation of Guo et al. (2011) and make mock catalogues for comparison with deep high-redshift surveys. Photometric properties are calculated with two different stellar population synthesis codes (Bruzual & Charlot 2003; Maraston 2005) in order to study sensitivity to this aspect of the modelling. The catalogues are publicly available and include photometry for a large number of observed bands from $4000\mathring{A}$ to 6μm, as well as rest-frame photometry and other intrinsic properties of the galaxies (e.g positions, peculiar velocities, stellar masses, sizes, morphologies, gas fractions, star formation rates, metallicities, halo properties). Guo et al. (2011) tuned their model to fit the low-redshift galaxy population but noted that at $z \geqslant 1$ it overpredicts the abundance of galaxies below the "knee" of the stellar mass function. Here we extend the comparison to deep galaxy counts in the B, i, J, K and IRAC 3.6μm, 4.5μm and 5.8μm bands, to the redshift distributions of K and 5.8μm selected galaxies, and to the evolution of rest-frame luminosity functions in the B and K bands. The B, i and J counts are well reproduced, but at longer wavelengths the overabundant high-redshift galaxies produce excess faint counts. At bright magnitudes, counts in the IRAC bands are underpredicted, reflecting overly low stellar metallicities and the neglect of PAH emission. The predicted redshift distributions for K and 5.8μm selected samples highlight the effect of emission from thermally pulsing AGB stars. The full treatment of Maraston (2005) predicts three times as many $z \sim 2$ galaxies in faint 5.8μm selected samples as the model of Bruzual & Charlot (2003), whereas the two models give similar predictions for K-band selected samples. Although luminosity functions are adequately reproduced out to $z \sim 3$ in rest-frame B, the same is true at rest-frame K only if TP-AGB emission is included, and then only at high luminosity. Fainter than $L_\star$ the two synthesis models agree but overpredict the number of galaxies, another reflection of the overabundance of $\sim 10^{10} M_\odot$ model galaxies at $z \geqslant 1$.

Key words: methods: numerical – methods: statistical – galaxies: formation – galaxies: evolution – stars: AGB

1 INTRODUCTION

Semi-analytic models of galaxy formation aim to predict the evolution of population properties such as the distributions of stellar mass, luminosity, star formation rate,

size, rotation velocity, morphology, gas content and metallicity, as well as the scaling relations linking these properties. They follow astrophysical processes affecting the baryonic components using a series of analytic, physically based models which are embedded either in an analytic representation (White & Frenk 1991; Kauffmann et al. 1993; Cole et al. 1994; Somerville & Primack 1999) or in a direct

⋆ E-mail:bhenriques@mpa-garching.mpg.de

numerical simulation (Kauffmann et al. 1999; Springel et al. 2001, 2005) of the evolution of the underlying dark matter distribution. Uncertain efficiencies and scalings of these astrophysical processes are represented by adjustable parameters. These may be set *a priori* through a detailed calculation or simulation of specific processes, or they may be determined observationally by matching suitably chosen data (e.g. Croton et al. 2006; Bower et al. 2006; Menci et al. 2006; Cattaneo et al. 2006; De Lucia & Blaizot 2007; Monaco et al. 2007; Somerville et al. 2008; Guo et al. 2011). The extremely broad range of relevant data and the considerable freedom in specifying appropriate recipes complicate the systematic comparison of semi-analytic models with data. New and robust statistical tools have recently been developed to facilitate quantitative comparisons (Kampakoglou et al. 2008; Henriques et al. 2009; Henriques & Thomas 2010; Bower et al. 2010; Lu et al. 2010).

Such comparisons are sensitive to stellar population synthesis models which are required both to derive intrinsic galaxy properties such as mass, age and star formation rate from observational data, and to calculate luminosities, colours and spectra for model galaxies. Erroneous conversions between physical and observable properties lead to incorrect conclusions about galaxy formation physics, so it is important to check the implications of adopting differing stellar populations synthesis models (e.g. Buzzoni 1989; Worthey 1994; Vazdekis et al. 1996; Fioc & Rocca-Volmerange 1997; Leitherer et al. 1999; Bruzual & Charlot 2003; Thomas et al. 2003; Maraston 2005; Conroy et al. 2009).

For example, the impact of including models for thermally-pulsating asymptotic giant branch (TP-AGB) stars has been studied in some detail in recent years. The contribution from these stars can significantly enhance the near-infrared emission of galaxies with Gyr-old populations (e.g. Maraston 1998; Maraston 2005; van der Wel et al. 2006, Marigo & Girardi 2007; Charlot & Bruzual 2007; Conroy et al. 2009). The data of Conroy et al. (2009) and Zibetti et al. (2009) show that inclusion of this additional emission can reduce the masses inferred from K-band light by as much as 0.6 dex. The semi-analytic models of Tonini et al. (2009, 2010), Fontanot & Monaco (2010) and Henriques et al. (2010) suggest that a substantial contribution from TP-AGB stars, as predicted by the model of Maraston (2005) may explain the large number of extremely red objects found at $z \sim 2$. Other examples of how uncertainties in stellar evolution modelling affect physical inferences from data are given by Conroy et al. (2010). Here we compare predictions of the Guo et al. (2011) semi-analytic model for two different population synthesis models, the one originally used by these authors (from Bruzual & Charlot 2003) and that of Maraston (2005).

Even neglecting uncertainties from stellar population modelling, mass-to-light ratios and other physical properties are often poorly constrained by available data. Estimates rely on fitting theoretical models to observed photometry and spectral energy distributions (SEDs) and approximately equivalent fits can often be obtained for broad ranges of assumed star formation history, chemical enrichment history and obscuration by dust. Additional uncertainties arise from possible variations in the initial mass function (IMF) with

which stars form, and from possible spectral contributions from an active galactic nucleus (AGN). It has been argued in the past that a single optical colour (e.g. $g - i$) is, in practice, sufficient to derive light-to-mass ratios accurate to 0.1 dex for most galaxies (Bell et al. 2003; Gallazzi & Bell 2009). However, Zibetti et al. (2009) showed that this is only true for relatively weak obscuration. For heavily obscured young populations, resolved photometry is needed to achieve an accuracy better than 0.2 dex and even that requires an additional near-infrared colour (e.g. one may combine $g - i$ and $i - H$).

Galaxy formation models directly predict star formation and enrichment histories, so in the absence of obscuration a well defined SED can be predicted for each galaxy as a superposition of simple stellar populations (SSPs), each made up of coeval stars of a single metallicity. The "observed" photometry is then easily obtained by redshifting the SED and integrating over the appropriate photometric filter functions. In practice, however, the conversion to observables is heavily influenced by dust and is sensitive to the details of its distribution within a galaxy (e.g. Granato et al. 2000; Cole et al. 2000). This significantly limits the precision with which observables can be predicted from galaxy formation models. Current semi-analytic models often attempt to handle these uncertainties by using observational data to constrain the dust model (e.g. Granato et al. 2000; Cole et al. 2000; Kitzbichler & White 2007; Guo & White 2009).

Because of such difficulties it seems wise to compare theory and observation for a broad range of properties, at different redshifts, and at different "conversion levels". The latter is particularly crucial at high-redshift, where very limited data are available and the relations between mass, light and star-formation rate are very uncertain. There is no preferred "comparison frame" and conclusions are convincing only if a consistent picture emerges which matches smoothly onto the lower redshift galaxy populations. Guo et al. (2011) compare their model extensively to low-redshift galaxies but only present limited predictions at high redshift. Specifically, they compare to published estimates of the evolution of the stellar mass function of galaxies out to $z \sim 4$, finding significant discrepancies for stellar masses below $5 \times 10^{10} \, \mathrm{M}_\odot$.

In this paper we extend this comparison considerably, analyzing the photometric properties of galaxies from high redshift to the present day, and comparing with observations at a variety of levels from number counts as a function of apparent magnitude, through redshift distributions of magnitude limited samples, to rest-frame luminosity functions as a function of redshift. In particular, we study predictions for the near-infrared bands for which data have recently become available from the Spitzer satellite. To facilitate this work we build lightcones using the MoMaF software (Blaizot et al. 2005). We are then able to reproduce the observational selection criteria of modern surveys such as the UKIRT Infrared Deep Sky Survey (UKIDSS) (Lawrence et al. 2007), the VIMOS-VLT Deep Survey (VVDS) (Le Fèvre et al. 2005), the Deep Evolutionary Exploratory Probe 2 Galaxy Redshift Survey (DEEP2) (Davis et al. 2003) or the Cosmic Evolution Survey (COSMOS) (Scoville et al. 2007).

Similar studies were performed by Kitzbichler & White (2007), Guo & White (2009) and de la Torre et al. (2011) for earlier versions of the Munich semi-analytic model. The

results here are based on the model of Guo et al. (2011) which is implemented simultaneously on the Millennium and Millennium-II Simulations and was retuned to fit a broad range of "high precision" data on the low-redshift galaxy population, primarily from the Sloan Digital Sky Survey (SDSS). We also expand the photometric coverage from the ultraviolet to IRAC bands and test the dependence on stellar population synthesis modelling over this wavelength range. In a recent paper, Somerville et al. (2011) compared a different semi-analytic model with photometry extending to even longer wavelengths (the far infrared). This required modelling the re-emission of starlight by heated dust, as also considered by Granato et al. (2000), Cole et al. (2000), Baugh et al. (2005), Lacey et al. (2010). Here we avoid this complication and compare only to directly observed starlight.

This paper is organized as follows. In Section 2 we summarize the characteristics of the semi-analytic model we use and we describe how we construct lightcones for it. Section 3 then presents results for number counts and redshift distributions as a function of apparent magnitude, and for rest-frame B- and K-band luminosity functions as a function of redshift. In Section 3 we present our conclusions.

2   THE SEMI-ANALYTIC MODEL

Modern semi-analytic models are built on merger trees from high-resolution dark matter simulations. These provide a description of the evolution of the mass and number density of dark matter halos and the subhalos within them, as well as of their spatial and kinematic distributions. The evolution of the baryonic components hosted by these (sub)halos is then followed using a set of simplified formulae describing each of the relevant astrophysical processes. The latest version of the Munich model (Guo et al. 2011) is implemented on two very large dark matter simulations, the Millennium Simulation (MS; Springel et al. 2005) and the Millennium-II Simulation (MS-II; Boylan-Kolchin et al. 2009). The MS follows the evolution of structure within a cube of side $500h^{-1}$Mpc (comoving) and its merger trees are complete for subhalos above a mass resolution limit of $1.7 \times 10^{10}h^{-1}$M$_\odot$. The MS-II follows a cube of side $100h^{-1}$Mpc but with 125 times better mass resolution (subhalo masses greater than $1.4 \times 10^8 h^{-1}$M$_\odot$). Both adopt the same WMAP1-based cosmology (Spergel et al. 2003) with parameters $h = 0.73, \Omega_m = 0.25, \Omega_\Lambda = 0.75, n = 1$ and $\sigma_8 = 0.9$. These are outside the region preferred by more recent analyses (in particular, σ_8 appears too high) but this is of no consequence for the issues we study in this paper. For consistency, we will use this cosmology whenever it is necessary to derive the physical properties of galaxies from observed fluxes and redshifts. The distributions of physical properties converge in the two simulations for galaxies with $10^{9.5}$M$_\odot < M_\star < 10^{11.5}M_\odot$. In this study we focus only on results from the MS, since its resolution limit is well below the stellar masses covered by the datasets with which we compare.

2.1   The model of Guo et al. 2011

For a full description of the semi-analytic model used in this work we refer the reader to Guo et al. (2011). Here we briefly describe changes from earlier versions of the Munich semi-analytic model that significantly affect our results.

Following Kitzbichler & White (2007) and Guo & White (2009), the model of Guo et al. (2011) includes a redshift-dependent model for internal extinction which assumes that the dust-to-gas ratio increases with metallicity but decreases with redshift. The effective optical depth is given by:

$$\tau_\lambda = \left(\frac{A_\lambda}{A_v}\right)_{Z_\odot} (1+z)^{-0.4} \left(\frac{Z_{\rm gas}}{Z_\odot}\right)^s \left(\frac{\langle N_H \rangle}{2.1 \times 10^{21}\,{\rm atms\,cm^{-2}}}\right), \quad (1)$$

where $\langle N_H \rangle$ represents the mean column density of hydrogen, $(A_\lambda/A_v)_{Z_\odot}$ is the extinction curve for the solar metallicity taken from Mathis et al. (1983) and $s = 1.35$ for $\lambda < 2000$ Å and $s = 1.6$ for $\lambda > 2000$ Å.

When they implemented the De Lucia & Blaizot (2007) version of the Munich model on the high-resolution Millennium-II Simulation, Guo et al. (2011) found it to over-produce dwarf galaxies. The authors therefore increased the efficiency of supernova feedback by introducing a direct dependence of the amount of gas reheated and ejected on the virial mass of the host halo. However, although the resulting model fits the stellar mass function of galaxies well at low redshift, it still produces more low-mass galaxies than are observed at $z > 1$. This deficiency is reflected in our results below.

Finally, Guo et al. (2011) introduced a more realistic treatment of satellite galaxy evolution and of mergers. The hot gas content of satellite galaxies is gradually stripped instead of being instantaneously removed at infall, as suggested by the simulations of McCarthy et al. (2008). This allows satellites to continue forming stars for a longer period and reduces the excessively rapid reddening of these objects. In addition, satellites of satellites remain connected to their parent galaxies and can merge with them, rather than being automatically reassigned to the central galaxy of the group or cluster. The model also includes a treatment of the tidal disruption of satellite galaxies.[1]

2.2   Lightcone Construction

At high redshift, the observed fluxes at a limited number of wavelengths are often the only data available for a galaxy, so that its redshift must be inferred through comparison of the observed colours to model templates. Even rest-frame magnitudes, colours and luminosities can then be subject to substantial uncertainties, and the conversion to intrinsic properties such as masses and star formation rates is problematic. Results not only depend on the accuracy of the photometric redshift, but are also (almost) degenerate with respect to the star formation history, metallicity and dust content of the galaxy. These quantities are direct predictions

---

[1] See Henriques & Thomas (2010) for an alternative extension of the Munich semi-analytic model modifying supernova feedback and including tidal disruption of satellites.

of a semi-analytic model, so that the conversion from intrinsic to observed properties is, in principle, well defined, given a stellar population synthesis model, an assumed IMF and a specific model for intrinsic obscuration. It is thus often convenient to consider conversion uncertainties as part of the model and to compare theoretical predictions directly with observables. To do this, we construct lightcones which allow the models to be "observed" in a way that mimics real surveys as directly as possible. We use two different population synthesis models to predict observables in order to assess the impact of the differing mass-to-light conversions they imply. We compute observed- and rest-frame fluxes from the ultraviolet to the near infrared so that our theoretical datasets resemble those of modern observational surveys not only in volume, but also in wavelength coverage.

Our lightcones are built using the Mock Map Facility (MoMaF) developed by Blaizot et al. (2005). We refer the reader to the original paper for a full description of the method. Here we briefly summarize the complications that arise when building lightcones from simulations of limited size and resolution.

The Millennium Simulation has side of $500h^{-1}$ Mpc (comoving). This is considerably smaller than, for example, the comoving distance to a galaxy observed at $z \sim 2$. Periodic replication of the simulation can lead to multiple appearances of the same object within the lightcone, although typically at different redshifts and so with different properties and at offset positions (due to large-scale motions). Blaizot et al. (2005) suggested applying a series of transformations (rotations, translations and inversions) when tiling space with periodic replications. This does not, of course, prevent multiple appearances of a given object within the lightcone, but these duplicates are then viewed from different directions and no longer fall on a (nearly) regular lattice.

Unfortunately, this technique also introduces discontinuities in large-scale structure at the boundaries between replications, affecting clustering statistics in a way which is at least as difficult to model as that of the original periodicity. Kitzbichler & White (2007) showed that for lightcones of relatively small solid angle, the central line-of-sight can be chosen to pass through the lattice of periodic replications in such a direction that multiple images of the same object are minimised or eliminated altogether. The latter is not possible if the comoving volume of the lightcone exceeds that of the simulation, but this technique can still be used to ensure that multiple appearances occur as far apart as possible both on the sky and in redshift. We therefore use the method of Kitzbichler & White (2007) in this paper. Space is filled with periodic replications of the simulation, a position is chosen for the observer, and the central line-of-sight of the survey field is given a previously chosen orientation. Galaxies whose positions intercept the lightcone are selected and their comoving distance is converted into a redshift.

As explained in Kitzbichler & White (2007), the time between stored snapshots for the Millennium Simulation varies between 100 and 380 Myr. This means that the intrinsic properties of galaxies are not generally available at the time corresponding to their comoving distance. Rather they must be taken from the stored snapshot which is closest in distance to their light-cone position. Hence, galaxies with comoving distance $(D_i + D_{i+1})/2 > D > (D_i + D_{i-1})/2$ are assigned the physical properties stored at z_i. The re-

sulting discontinuity in galaxy population properties, at the boundaries between snapshots, could be reduced by interpolating, but this works poorly for positions and velocities since the output separation is comparable to orbital times within groups and clusters. Moreover, it is not straightforward for other galaxy properties either since these change discontinuously on timescales shorter than the output spacing, for example through mergers and starbursts. We thus follow Kitzbichler & White (2007) and do not attempt any interpolation.

The *apparent* luminosities and colours of galaxies depend strongly on their redshifts through the conversion between rest- and observed-frame photometric bands and through the inverse square dependence of apparent luminosity on distance. As explained in Kitzbichler & White (2007) the final redshift of the galaxy in the lightcone is not available at the time observed-frame luminosities are computed in the semi-analytic model. However, there will be two extreme redshifts that bracket it. We compute apparent observed-frame luminosities (for fixed intrinsic properties) using these upper and lower limits, and once the galaxy is placed in the lightcone, we interpolate to obtain final observed-frame quantities.

For this paper we construct lightcones for square areas of 1.4×1.4 deg^2 out to high redshift with no faint magnitude cut. They are however limited by the mass resolution of the dark matter simulation ($1.7 \times 10^{10} h^{-1} M_\odot$ in halo mass) corresponding to stellar masses of $\sim 10^{9.5} M_\odot$ at z=0. While this does not matter for the questions we study in this paper, it should be borne in mind if the lightcones are used for other purposes.[2]

2.3   Stellar Populations and Photometry

2.3.1   *Stellar Population Synthesis Models*

Semi-analytic models predict intrinsic properties of galaxies, such as stellar mass, star formation history, gas and dust content and metallicity. In order to convert these into observed spectral energy distributions (SED) or broad-band photometry, evolutionary population synthesis and dust models are required. The former predict the evolution of the light associated with a single short burst of star formation of given metallicity and with an assumed Initial Mass Function (IMF), a so-called Simple Stellar Population (SSP). The intrinsic stellar emission from a model galaxy is then represented as a superposition of SSPs weighted according to its star formation history. This emission must be processed through a dust model in order to predict the observable stellar emission. Uncertainties in the conversion between mass and light can jeopardise any comparison between theory and observations. There are still significant differences between published evolutionary population synthesis models and these should be considered as part of the systematic uncertainties when comparing semi-analytic model predictions to data. Throughout this paper we present results from two distinct stellar population synthesis codes: one that has been traditionally used in the Munich model (Bruzual & Charlot

---
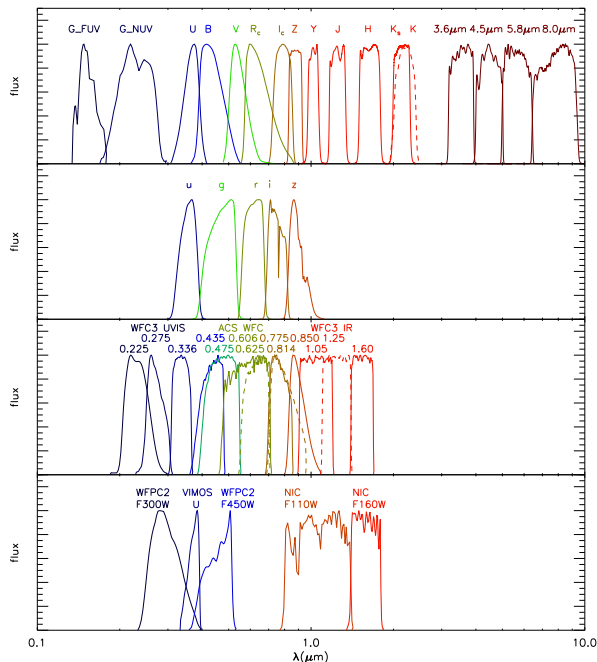
Figure 1. The response functions of the filters for which fluxes are computed for the lightcones produced in this paper. These extend from the far ultra-violet to the IRAC bands and include: in the top panel, GALEX FUV and NUV, Johnson $UBVR_cI_cJHK_sK$ and IRAC bands; in the second panel, SDSS $ugriz$; in the third panel, HST WFC3 UV and IR and ACS WFC; and in the bottom panel, HST WFPC2, VIMOS U and NICMOS.

2003) and the Maraston (2005) model implemented in the semi-analytic code by Henriques et al. (2010). In both cases we adopt the same Chabrier (2003) IMF and a similar metallicity grid. We hope that the differences we find will give some indication of the impact of mass-to-light conversion uncertainties on galaxy formation modelling.

2.3.2   Photometry

In order to increase the predictive power of the model and allow it to be tested against a wider range of observations, we also expand the number of photometric bands for which fluxes are computed, covering all wavelengths dominated by direct emission from stars, from the UV to the near-infrared IRAC bands. In Fig. 1 we plot the relevant filter transmission curves. In the top panel we show the GALEX FUV and NUV, the Johnson $U, B, V, R_c, I_c, Z, Y, J, H, K_s, K$ and the IRAC 3.6μm, 4.5μm, 5.8μm and 8.0μm bands; in the second panel, the SDSS u, g, r, i, z bands; in the third panel, bands from HST instruments, three UV bands from the WFC3-UVIS (0.225μm, 0.275μm, 0.336μm), seven optical bands from the ACS-WFC (0.435μm, 0.475μm, 0.606μm, 0.625μm, 0.775μm, 0.814μm, 0.850μm) and three near-infrared bands from the WFC3-IR (1.05μm, 1.25μm, 1.60μm); and in the bottom panel, the VIMOS U band, the 2 NICMOS near-infrared bands (1.1μm and 1.6μm) and two WFPC2 bands (0.30μm and 0.45μm). While we will not give results for all these bands in this paper, we will include the relevant ap-

parent magnitudes in our light-cone catalogues in order to enhance their utility to others.

All magnitudes are in the AB system. In order to be as close as possible to observations, we use the K_s-band when presenting results for number counts and redshift distributions and the K-band when discussing the evolution of the rest-frame luminosity function.

The lightcones constructed and made public in this work provide a useful tool to test observational derivations of intrinsic galaxy properties. The wide wavelength coverage of observed- and rest-frame photometry, together with the two stellar population synthesis models considered, can be used to check derivations of rest-frame magnitudes from observed photometry, as well as the reliability of properties obtained from SED fitting, such as stellar masses, ages and star-formation histories.

3   RESULTS

In this section we compare predictions of our models to observational data. We start with number counts as a function of apparent magnitude in a wide range of photometric bands (from the optical blue to the IRAC bands) and move on to redshift distributions for K and IRAC 5.8μm selected galaxies. Finally we investigate the evolution of the rest-frame optical and near-infrared luminosity functions which, although further from the directly observed quantities, allow a better understanding of galaxy evolution.

Kitzbichler & White (2007) and de la Torre et al. (2011) presented similar tests for an earlier version of the Munich semi-analytic model. Here, we take advantage of recent advances in the available observations and extend these comparisons to higher redshift and to a wider range of wavelengths. We also test the impact of population synthesis models by comparing results for the Bruzual & Charlot (2003) and the Maraston (2005) models. This follows up work by Tonini et al. (2009, 2010); Fontanot & Monaco (2010) and Henriques et al. (2010), who showed that the inclusion of near-infrared emission from TP-AGB stars increases the predicted number of massive and extremely red objects at $z \sim 2$, as seems to be required by observation. Our comparison is based on a large number of lightcone realizations with areas and selection effects matching the relevant observational surveys.

3.1   Number Counts

Galaxy counts in a given observed band can be difficult to interpret. At each apparent magnitude they consist of galaxies at a wide range of redshifts and thus with correspondingly wide ranges of absolute magnitude and of emitted wavelength. Nevertheless, such counts provide an important test of models because they are directly observed and so are independent of uncertainties in redshift, k-correction, obscuration correction, etc.

Fig. 2 shows galaxy number counts for the B and i, J, K_s, IRAC 3.6μm, 4.5μm and 5.8μm bands (from top left to bottom right). Solid red and dashed blue lines are model predictions for the Maraston (2005) and Bruzual & Charlot (2003) stellar population synthesis models respectively. Filled regions show the 1σ field-to-field scat-
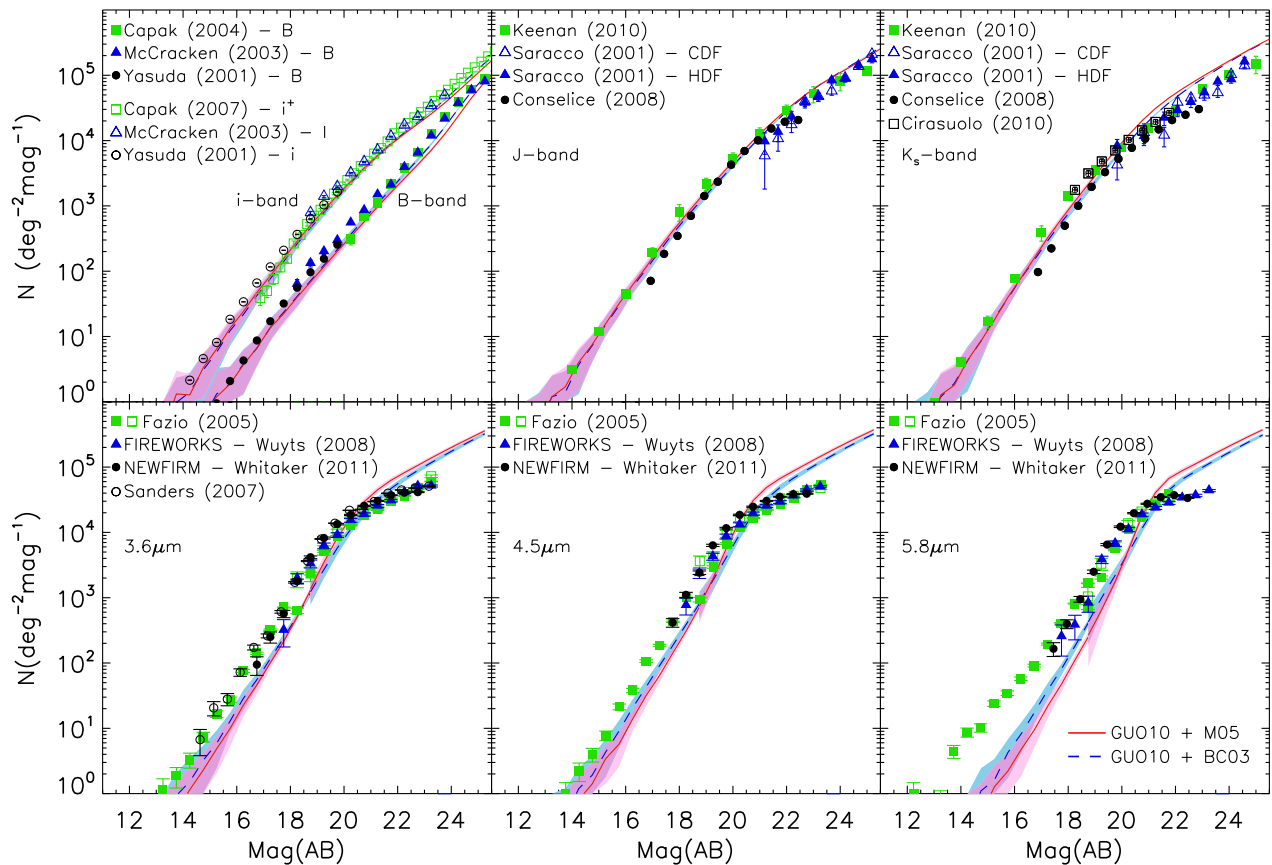
Figure 2. Galaxy number counts as a function of apparent magnitude. From top left to the bottom right, the panels show number counts in the B and i, J, K_s, IRAC 3.6μm, 4.5μm and 5.8μm bands. Theoretical predictions for the Maraston (2005) and Bruzual & Charlot (2003) population synthesis models are shown as solid red and dashed blue lines respectively. The filled regions represent the 1σ field-to-field scatter for surveys of area 2 deg^2, except for the IRAC bands at faint magnitudes (M>18.5) where 100 arcmin^2 fields are assumed. The B-band number counts are compared with data from SDSS (Yasuda et al. 2001), VVDS (McCracken et al. 2003) and HDF-N (Capak et al. 2004); i-band counts are also compared with data from SDSS and VVDS and with the COSMOS sample (Capak et al. 2007); for the J- and K_s- bands we show observations from the CDF and HDF-S (Saracco et al. 2001), DEEP2 and Palomar (Conselice et al. 2008) and MOIRCS (Keenan et al. 2010) with UKIDSS-UDF data (Cirasuolo et al. 2010) plotted for the K-band; Spitzer (Fazio et al. 2004), FIREWORKS (Wuyts et al. 2008) and NEWFIRM (Whitaker et al. 2011) data are shown for the IRAC$_{3.6\mu m}$, IRAC$_{4.5\mu m}$ and IRAC$_{5.8\mu m}$ bands.

ter expected among surveys of area 2 deg^2, except that 100 arcmin^2 fields are assumed for the IRAC bands at faint magnitudes (M>18.5).

The optical B- and i-band number counts are compared with data from the Sloan Digital Sky Survey (SSDS; Yasuda et al. 2001) and the Vimos Very Deep Survey (VVDS; McCracken et al. 2003) at brighter magnitudes. At fainter magnitudes we use the Hubble Deep Field - North (HDF-N; Capak et al. 2004) for the B-band and the COS-MOS sample (Capak et al. 2007) for the i-band. Both population synthesis models match the data for bright galaxies (seen at low redshift in the rest-frame optical), while the Bruzual & Charlot (2003) model predicts more galaxies at faint apparent magnitudes, in better agreement with observations. Similar trends were found for previous versions of the Munich semi-analytic model (Kitzbichler & White 2007; de la Torre et al. 2011). It is difficult to draw firm conclusions from this result, however, since these faint counts cor-

respond to rest-frame ultra-violet emission from galaxies at high redshift where uncertainties affect not only the stellar population modelling, but also the simplistic treatments of starbursts and of dust obscuration in the semi-analytic model. Conroy et al. (2010) showed, for example, that increasing the number of blue stragglers or blue horizontal branch stars increases the predicted ultra-violet emission from passive galaxies.

We compare the J- and K_s-band counts to observations from the Chandra Deep Field and the Hubble Deep Field - South (CDF and HDF-S; Saracco et al. 2001) from the DEEP2 and Palomar surveys (Conselice et al. 2008), and from the MOIRCS sample (Keenan et al. 2010) . In addition, we show K-band counts based on the UKIDSS-Ultra Deep Field data (UKIDSS-UDF; Cirasuolo et al. 2010). The two stellar population synthesis models give similar predictions for the J-band number counts which agree with the data. Both predict too many faint objects in the K_s and K

bands. As shown by Guo et al. (2011), and as this paper will clarify, this is because the semi-analytic model overpredicts the abundance of low-mass galaxies at high redshift. The two stellar population synthesis models predict similar counts at both bright (low redshift, near infrared emission) and faint (high redshift, red optical emission) apparent magnitudes, but they disagree at intermediate apparent magnitudes. As we will see in more detail below, the difference is a consequence of TB-AGB emission from stars with ages of one or two Gyr which is fully included in the Maraston (2005) but not in the Bruzual & Charlot (2003) stellar population model.

Predicted number counts for the IRAC 3.6μm, 4.5μm and 5.8μm bands are plotted against Spitzer (Fazio et al. 2004), FIREWORKS (Wuyts et al. 2008) and NEWFIRM (Whitaker et al. 2011) observations. Both the models and the observations show a pronounced change in slope at an apparent magnitude near 20, but the break is stronger in the observations than in the model and occurs at slightly brighter apparent magnitudes. As a result, the models under-predict the number of bright objects (low redshift, emission longwards of the rest-frame K-band) and over-predict the number of faint objects (high redshift, emission in the rest-frame JHK region). The latter underprediction is even more pronounced here than in the K-band and again is likely due to the overabundance of lower mass galaxies at $z \geqslant 1$ in the model. The deficit of bright galaxies is visible also in the $z = 0$ rest-frame K-band luminosity function (Fig. 5). Since Guo et al. (2011) tuned their semi-analytic model to match the observed low-redshift stellar mass function, this deficit implies overly large mass-to-near-infrared-light ratios which might be explained by overly small stellar metallicities. Indeed, Henriques & Thomas (2010) showed that the most massive low-redshift galaxies in the De Lucia & Blaizot (2007) version of the model have stellar metallicities which are too low by about a factor of two (the dashed red lines in their Figs 4 and 10). An increase in metallicity could remove the discrepancy by reducing the mass-to-near-infrared-light ratios in model.[3] Another important factor, particularly for the IRAC 5.8μm band, is the possible contamination by emission from hot dust, specifically, emission in the 3.3, 6.2 and 7.7μm PAH features (Draine et al. 2007; Draine & Li 2007; da Cunha et al. 2008). Such emission is not included in the models but may well be significant in the real low-redshift galaxies.

3.2 Redshift distributions for K and IRAC$_{5.8\mu m}$ selected samples

In Fig. 3 we compare predictions from our models to the observed photometric redshift distributions of galaxy samples selected above K_s and IRAC 5.8μm apparent magnitude limits. As for the number counts, the solid red and dashed blue lines represent predictions based on the Maraston (2005) and Bruzual & Charlot (2003) stellar population synthesis models. Filled regions show the expected
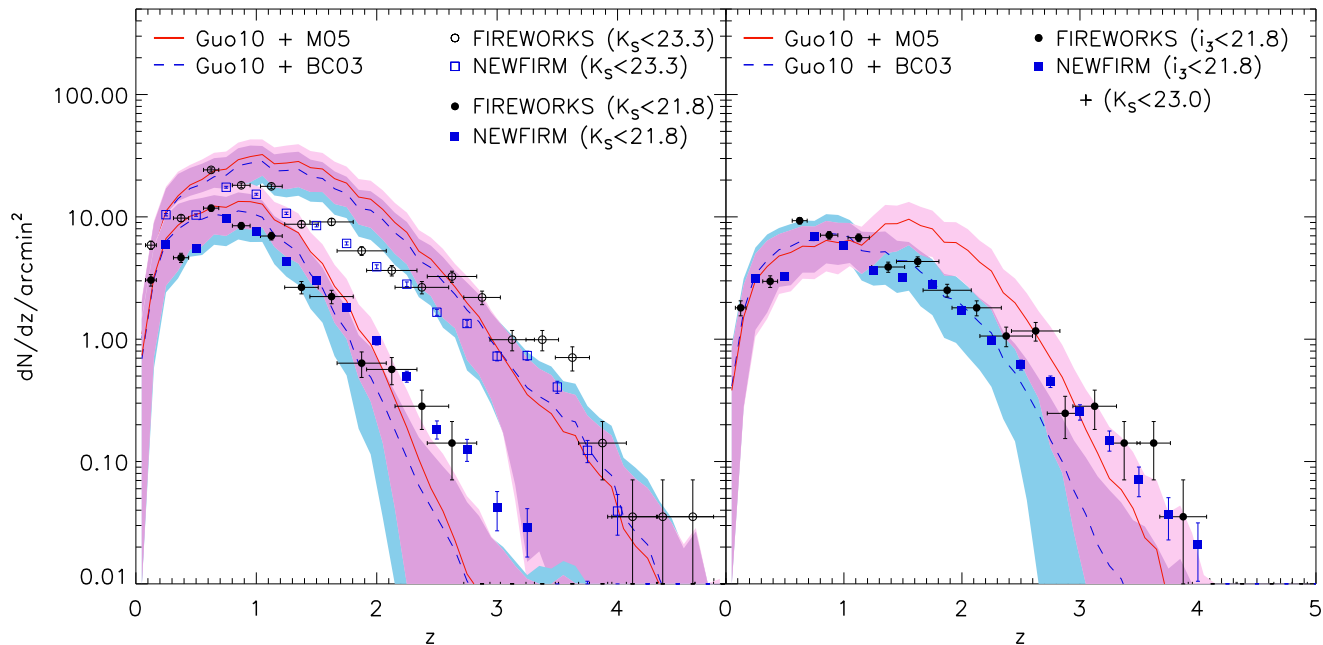
1σ scatter among fields with an area of 100 arcmin^2. In the left panel the number of galaxies per unit area and redshift is plotted for samples with $K_s < 21.8$ and $K_s < 23.3$, while the right panel gives similar results but for samples with IRAC 5.8μm apparent magnitude brighter than 21.8 (and $K_s < 23.0$). Our theoretical predictions are compared with data from two public catalogues: the FIREWORKS data for the GOODS-CDF (Wuyts et al. 2008) and the NEWFIRM Medium Band Survey data for the COSMOS and AEGIS fields (Whitaker et al. 2011). The wide photometric coverage of these two datasets results in robust and relatively precise photometric redshift measurements. Our theoretical samples are selected using photometric criteria very similar to those defining the observed samples, although we plot the distribution of their true redshifts rather than attempting to reproduce the observational redshift estimation procedure.

Selection by observed-frame K_s-band magnitude picks galaxies on the basis of their rest-frame K-band emission at low redshift, their rest-frame J band emission at $z \sim 1$, and their rest-frame optical emission at $z > 1.5$. For both magnitude limits, the samples are dominated by intrinsically faint objects at low-redshift but by intrinsically bright galaxies beyond $z \sim 1$ (for $K_s < 21.8$) or $z \sim 1.5$ (for $K_s < 23.3$)). For both apparent magnitude limits the predictions for the two population synthesis models agree, and for the brighter limit they are consistent with the observations out to a redshift of almost two. Both underpredict the counts at higher redshift, with the effect being slightly larger for the Bruzual & Charlot (2003) model. This may reflect an underabundance of intrinsically bright objects (in the optical) in the model at these redshifts, but could also be due to magnitude and photometric redshift errors in the data which primarily affect the tails of the distribution. For the fainter apparent magnitude limit the model clearly overestimates the number of objects over the redshift range $1 < z < 2.5$. These galaxies typically have stellar masses of order a few $10^{10} M_\odot$ and this discrepancy reflects the overabundance of objects of this mass and redshift unity that was flagged by Guo et al. (2011). The same problem was identified in earlier versions of the model by Kitzbichler & White (2007) and de la Torre et al. (2011). At higher and lower redshifts the abundances agree quite well in model and data, reflecting the fact that the semi-analytic model was tuned to fit galaxy abundances at low redshift, and predicts an abundance of high-mass galaxies which fits observed estimates quite well at high redshift.

For the IRAC 5.8μm selected samples shown in the right panel of Fig. 3, there is a significant difference between the predictions of the two population synthesis models. While the Bruzual & Charlot (2003) model predicts a distribution with similar shape to those in the left panel, the Maraston (2005) model makes a concordant prediction only at $z < 1.2$. Beyond this point there is a "bump" and at higher redshift it predicts roughly 3 times as many galaxies as the Bruzual & Charlot (2003) model. A corresponding bump is not present in the observational data which are better described by the Bruzual & Charlot (2003) model, at least out to $z \sim 2.5$. The bump in the Maraston (2005) model is caused by strong rest-frame JHK emission from TP-AGB stars associated with intermediate age stellar populations. While this emission brings the predicted numbers of galaxies into rough agreement with the data at the high-

---

[3] The luminosity correction depends on the actual deficit in metallicity, which in turn depends strongly on which stellar population model is used to derive masses and metallicities for the observed galaxies.

Figure 3. The redshift distribution of galaxies selected above observed-frame K_s-band (left panel) and IRAC 5.8μm-band (right panel) apparent magnitude limits. The solid red and dashed blue lines represent the mean predictions of our semi-analytic model for the Maraston (2005) and Bruzual & Charlot (2003) stellar population synthesis models. The filled regions show the 1σ scatter among fields with area 100 arcmin^2. The left panel shows the total number of galaxies per unit area and redshift for samples with $K_s < 21.8$ and $K_s < 23.3$. Similar curves are shown in the right panel but for samples with IRAC$_{5.8\mu m}$ <21.8 and K_s <23.0. Theoretical distributions are compared with data from FIREWORKS (Wuyts et al. 2008) and from the NEWFIRM Medium Band Survey (Whitaker et al. 2011).

est redshifts, it results in an overabundance at $z \sim 2$ where the observational datasets appear most robust. Since this effect is also present for data in other wavebands, for which TP-AGB emission is not an issue, it suggests that it results from the semi-analytic model overpredicting the abundance of the relevant moderate mass galaxies by a substantial factor at this redshift. In view of this, the agreement achieved by the Bruzual & Charlot (2003) model is probably coincidental, resulting from the overestimated abundance of moderate mass galaxies being compensated by an overestimate of their rest-frame JHK mass-to-light ratios.

3.3   The rest-frame B-Band Luminosity Function

Rest-frame luminosity functions and colour distributions as a function of redshift provide direct estimates of the abundance evolution of various galaxy types (e.g. star-forming/passive, high/low mass). However, they require accurate redshifts and appropriate photometry if they are to be determined reliably from observed-frame fluxes. The wide wavelength coverage of modern surveys produces robust photometric redshifts, and, in addition, allows rest-frame optical and near-infrared magnitudes to be determined by interpolation over the full range $0 < z < 4$, rather than requiring an uncertain extrapolation based on an SED fit.

Guo et al. (2011) showed that their semi-analytic model reproduces observed $z \sim 0.1$ luminosity functions in the SDSS g, r, i and z bands. At higher redshift they implemented the redshift-dependent dust model of Kitzbichler & White (2007). This reproduces the observed

abundance of colour-selected galaxies at $z \sim 2$ and $z \sim 3$ for the previous version of the semi-analytic model (see Guo & White 2009). In Fig. 4 we show the evolution of the B-band luminosity function from $z = 0$ to $z = 3$ for our current semi-analytic model. Solid red and dashed blue lines, represent versions with the Maraston (2005) and Bruzual & Charlot (2003) stellar population models respectively. Filled regions give the expected 1σ field-to-field scatter for surveys of area 1.4 deg^2, except that smaller fields (with area 150 arcmin^2) were assumed for the $2.5 < z < 3.5$ panel, for the $1.3 < z < 2.0$ panel fainter than -21.0 and for the $0.8 < z < 1.2$ panel fainter than -19.0.

At $z \sim 0$ the model b_j-band luminosity function[4] is compared with the 6 Degree Field Galaxy Redshift Survey result of Jones et al. (2006, 6DFGRS), repeated for reference as a black dotted line in all panels. For the $z \sim 0$ panel we use the final snapshot of the simulation rather than the lightcone, finding excellent agreement with the 6DFRS result, just as was the case for the corresponding SDSS luminosity function (in the g band) in Guo et al. (2011). For the other $z \leqslant 1$ panels we compare with data from the relatively wide VVDS (Ilbert et al. 2005), DEEP2 (Willmer et al. 2006) and zCOSMOS (Zucca et al. 2009) surveys. At higher redshift only data for smaller fields are available. We show results from Poli et al. (2003, HDF-S), Giallongo et al. (2005, HDF-N), Marchesini et al. (2007, GOODS-MUSYC+FIRES) and Salimbeni et al. (2008, GOODS-MUSYC).

---

[4] We assume $b_j = B - 0.267(B - V)$, (Norberg et al. 2002).
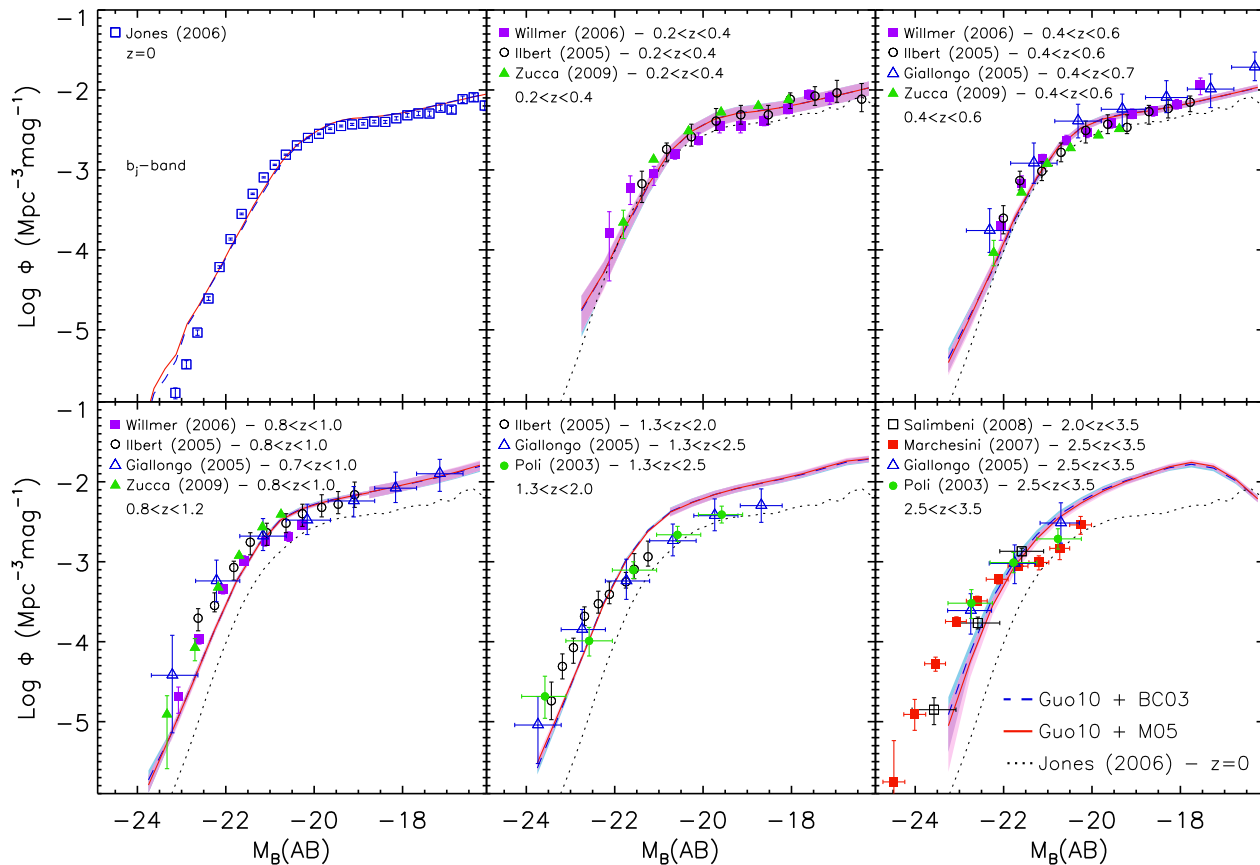
Figure 4. Evolution of the rest-frame B-band luminosity function from $z = 3$ to $z = 0$. Theoretical predictions for the Maraston (2005) and Bruzual & Charlot (2003) stellar population models are shown as solid red and dashed blue lines respectively. Filled regions represent the 1σ field-to-field scatter expected for surveys of area 1.4 deg^2, except in the highest redshift panel, where 150 arcmin^2 fields are assumed. Fields of this size are also assumed for the intrinsically fainter galaxies in the 0.8<z<1.2 and 1.3<z<2.0 panels (for galaxies with $M_B > -19.0$ and > -21.0 respectively). At $z = 0$ the model b_j-band luminosity function ($b_j = B - 0.267(B - V)$; Norberg et al. 2002) is compared with observations from the 6DFGRS (Jones et al. 2006), repeated at all redshifts as a dotted black line. At higher redshifts we show observational estimates from VVDS (Ilbert et al. 2005), DEEP 2 (Willmer et al. 2006), zCOSMOS (Zucca et al. 2009), HDF-S (Poli et al. 2003), HDF-N (Giallongo et al. 2005), GOODS-MUSYC plus FIRES (Marchesini et al. 2007) and GOODS-MUSYC (Salimbeni et al. 2008).

The model reproduces the evolution of the rest-frame B-band luminosity function reasonably well out to $z = 3$. It overpredicts the abundance of faint objects at $z \sim 2$ and underpredicts the abundance of bright objects at $z \sim 3$, although it may still be compatible with the data given the relatively large error bars quoted by the observers and the substantial scatter between the observational determinations. The two stellar population synthesis models give very similar results in this band. We note that the predicted fluxes are strongly affected by dust, and so are dependent on the adopted dust model. Further testing of the simplistic and relatively poorly motivated model of Kitzbichler & White (2007) is clearly needed.

3.4 The K-Band Luminosity Function

The K-band luminosity function has long been thought of as a proxy for the stellar mass function. Recent results have shown, however, that this assumption, while moder-

ately accurate at low redshift, can break down badly at early times. Notably, the fact that the characteristic luminosity $L_\star$ increases with increasing redshift just as for the optical bands (Cirasuolo et al. 2010) is inconsistent with a time-independent K-band mass-to-light ratio, which would imply the "evaporation" of material from the most massive galaxies. This luminosity function behaviour is easily understood in the context of recent stellar population synthesis models. In particular, a significant amount of K-band emission comes not from the old populations which dominate the stellar mass, but rather from intermediate age stars (~ 1 Gyr) passing through the TB-AGB phase (Maraston 2005; Charlot & Bruzual 2007). At high redshifts these relatively young populations can dominate the rest-frame luminosity in the K-band and they are only later replaced by predominantly old populations (Henriques et al. 2010).

In Fig. 5 we plot the evolution of the K-band luminosity function out to $z = 3$. As in previous figures, the solid red and dashed blue lines represent predictions based on
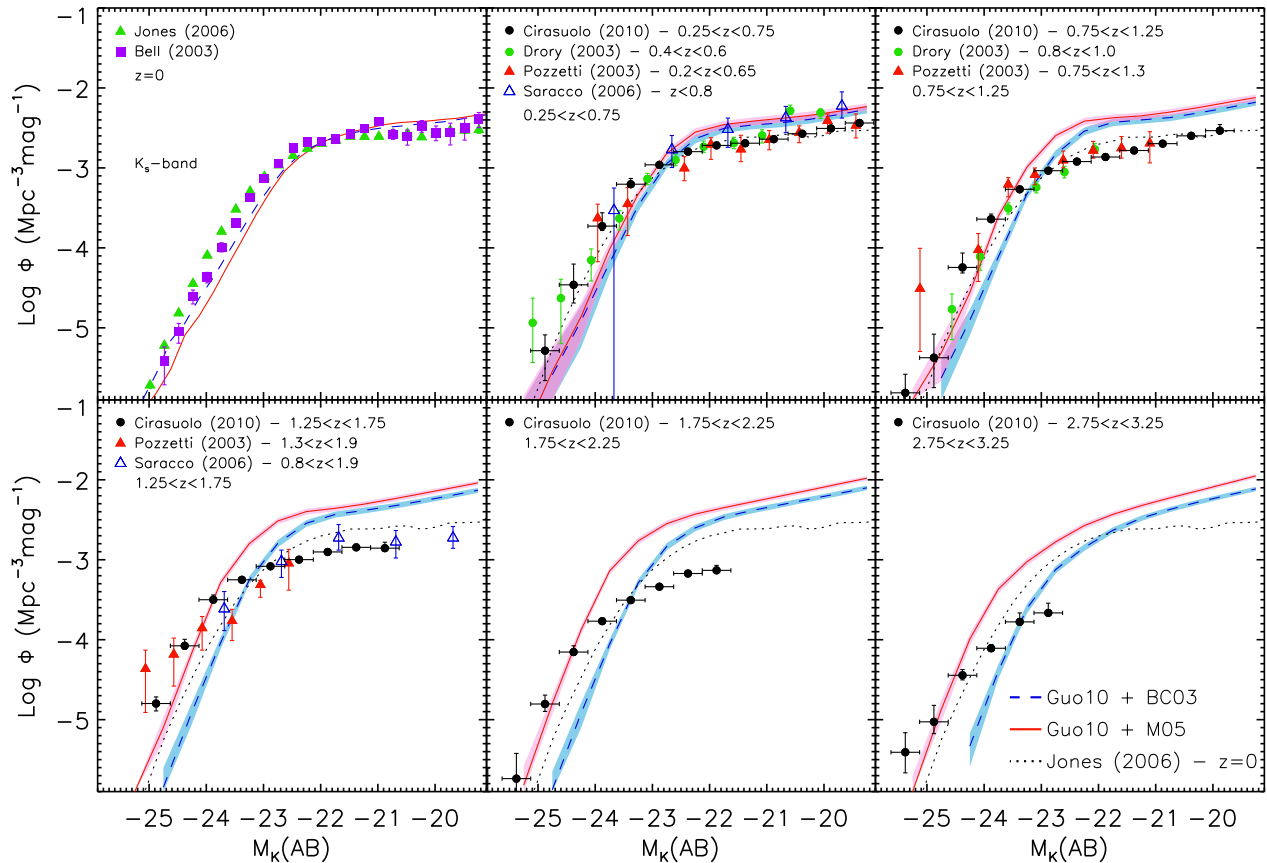
Figure 5. Evolution of the rest-frame K-band luminosity function from $z = 3$ to $z = 0$. Predictions of our semi-analytic model for the Maraston (2005) and Bruzual & Charlot (2003) population synthesis models are shown by solid red and dashed blue lines respectively. Filled regions represent the expected 1σ field-to-field scatter for surveys of area $0.7 \ \mathrm{deg}^2$. At $z \sim 0$ the model K_s-band luminosity function is compared with data from 2MASS (Bell et al. 2003) and 6DFGRS+2MASS (Jones et al. 2006). We repeat the latter at all redshifts as a black dotted line. At higher redshifts we show observational estimates based on MUNICS (Drory et al. 2003), the UKIDSS-UDF (Cirasuolo et al. 2010), the K20 Survey (Pozzetti et al. 2003) and the HDF-S (Saracco et al. 2006). Note that in all surveys other than the UKIDSS-UDF, the rest-frame K-luminosities are not directly measured but are rather estimated by extrapolating from the *observed frame K*-band fluxes using an SED model.

the Maraston (2005) and Bruzual & Charlot (2003) stellar population models, and filled regions outline the expected 1σ field-to-field scatter among surveys of area $0.7 \ \mathrm{deg}^2$. At $z \sim 0$ the model K_s-band luminosity function is compared with observational data from 2MASS (Bell et al. 2003) and 6DFGRS+2MASS (Jones et al. 2006). As a reference, we repeat the latter at all redshifts as a black dotted line. For the $z \sim 0$ panel we use the final snapshot of the simulation rather than the lightcone to obtain the theoretical prediction. At higher redshifts, the model is compared with data from the MUNICS (Drory et al. 2003), K20 (Pozzetti et al. 2003), HDF-S (Saracco et al. 2006) and UKIDSS-UDF Cirasuolo et al. (2010). Only the last of these surveys estimates the rest-frame K-band flux directly by interpolating between observed-frame magnitudes at corresponding wavelengths (from Spitzer/IRAC). The other surveys extrapolate the *observed-frame K* flux to longer wavelength using an uncertain SED fit and thus may be subject to substantial systematic errors.

Our two population synthesis models give very similar

predictions for the rest-frame K-band luminosity function out to $z \sim 0.5$. At higher redshifts their shapes and their normalisations remain similar but their characteristic luminosities diverge with the Maraston (2005) prediction being brighter by about 0.4, 0.5, 0.6 and 0.75 magnitudes at redshifts of 1.0, 1.5, 2.0 and 3.0 respectively. This reflects the increasing contribution from TP-AGB stars as the mean age of the galaxies gets younger. The predictions of both models are strongly at variance with observation at these redshifts. While the Maraston (2005) model agrees with the high-mass tail of the observed luminosity functions at all redshifts, it seriously overpredicts the abundance of less massive galaxies at $z = 1$ and earlier. For the lowest luminosity bin of the UKIDSS-UDF dataset the overprediction is by factors of 2, 4, 6 and almost 8 at redshifts of 1.0, 1.5, 2.0 and 3.0 respectively. The Bruzual & Charlot (2003) model fails to reproduce the rest-frame K luminosities of the most massive systems (by about 0.7 mag by $z \sim 3$) but nevertheless overpredicts the abundance of less luminous systems almost as badly as the Maraston (2005) model. This is the sub-

stantial problem already pointed out by Guo et al. (2011); their galaxy formation assumptions produce moderate mass galaxies ($M_\star \sim 10^{10} M_\odot$) too early to be compatible with current data on populations at $z \geqslant 1$.

As noted above when discussing Fig. 2, the model also slightly underestimates the K-band luminosities of massive low-redshift galaxies. This more subtle problem is due to these massive galaxies being too blue (see the colour distributions in Fig. 12 of Guo et al. 2011). This is likely caused by an underabundance of heavy elements (Henriques & Thomas 2010).

Similar results for the evolution of the rest-frame K-band luminosity function have been obtained for an earlier version of the Munich semi-analytic model (De Lucia & Blaizot 2007, as well as for the semi-analytic models of Menci et al. 2006, Monaco et al. 2007 and Fontanot et al. 2009). In a recent paper Somerville et al. (2011) compared another independent semi-analytic model to observational data on the evolution of the rest-frame $1500\mathring{A}$, B and K band luminosity functions. The authors were able to get a reasonable match to the bright tail without including TP-AGB emission, but they do obtain a much weaker evolution of the characteristic $L_\star$ than observed, in concordance with our Bruzual & Charlot (2003) results. They also overpredict the abundance of lower luminosity galaxies by very similar factors to those that we find here. It seems that whatever is causing the overly early formation of lower mass galaxies is common to all recent semi-analytic models.

4 CONCLUSIONS

We have constructed lightcones from the latest version of the Munich semi-analytic model (Guo et al. 2011) and used them to compare the model with the high-redshift galaxy population as revealed by recent deep surveys at optical and near-infrared wavelengths. We have combined the model with two different stellar population synthesis packages (Bruzual & Charlot 2003; Maraston 2005) in order to understand how differences in the photometric modelling are reflected in inferences about galaxy evolution. We use multiple independent lightcones to characterize cosmic variance uncertainties in currently available datasets. Our mock catalogues are made publicly available with publication of this paper and provide observer-frame photometry in 40 commonly used photometric bands, in addition to rest-frame photometry and a variety of physical properties of the galaxies (positions, peculiar velocities, stellar masses, halo masses, sizes, morphologies, gas fractions, star formation rates, metallicities, halo properties).

We now summarise the principal conclusions from our comparison of models and data.

• For both stellar populations the model matches the observed-frame B, i and J number counts but overpredicts the counts at faint magnitudes ($m_{AB} > 20$) in the K_s, IRAC 3.6μm, 4.5μm and 5.8μm bands. This reflects the overproduction of moderate mass galaxies (stellar masses $M_\star \sim 10^{10} M_\odot$) at $z \geqslant 1$ already noted by Guo et al. (2011). The matching of the faint optical counts is fortuitous – this overproduction is masked by overly large mass-to-light ra-

tios in the rest-frame near-UV, perhaps due to problems with the dust modelling.

• At bright magnitudes ($m_{AB} < 20$) the model underpredicts the counts in the three IRAC bands. This is due to an underestimation of the near-infrared luminosities of low-redshift massive galaxies caused in part by the fact that such galaxies are insufficiently metal-rich in the model, and in part by the model's neglect of PAH emission from hot dust (which is particularly significant at 5.8μm).

• At magnitudes where the model K_s-band counts agree with observations the redshift distribution of K_s-selected samples is also reproduced. At fainter magnitudes where the counts are overpredicted, the excess galaxies occur primarily at $1 < z < 2.5$, again reflecting the overproduction of $M_\star \sim 10^{10} M_\odot$ galaxies at these epochs. The two population synthesis models give similar results in both regimes.

• The two population synthesis models predict different redshift distributions for galaxies selected to $m_{AB} \sim 22$ in the IRAC 5.8μm band. Emission from TP-AGB stars enhances the number of galaxies at $z > 1.5$ in the Maraston (2005) model by about a factor of 3 relative to the Bruzual & Charlot (2003) model, causing it to overpredict the observed abundance at $z \sim 2$. Although the Bruzual & Charlot (2003) model agrees with the observed redshift distribution for $0 < z < 3$, this is a result of the overabundance of moderate mass galaxies being cancelled by an overestimate of their near-infrared mass-to-light ratios.

• The two population synthesis give similar results for the evolution of the rest-frame B-band luminosity function, agreeing well with observation out to $z = 1.2$. At higher redshift the agreement is less convincing. The overabundance of lower mass model galaxies starts to become evident, and there is some indication that the models underpredict the abundance of the most luminous objects. Cosmic variance and other uncertainties in the currently available data, together with dust modelling uncertainties in the model, preclude any strong conclusions.

• The Maraston (2005) population model reproduces the bright tail of the rest-frame K-band luminosity function all the way out to $z \sim 3$, whereas the Bruzual & Charlot (2003) model underpredicts the near-infrared luminosities of these massive galaxies by an amount which increases from about 0.3 mag at $z \sim 1$ to 0.7 mag at $z \sim 3$. The overproduction of $M_\star \sim 10^{10} M_\odot$ galaxies at these times causes both models to substantially overpredict galaxy abundances below the knee of the luminosity function.

In the literature it has often been suggested that semi-analytic models fail to reproduce the rest-frame K-band galaxy luminosities of the brightest high-redshift galaxies (at $z \sim 2 - 3$), and the failure is usually attributed to insufficiently rapid mass growth at early times (Pozzetti et al. 2003; Cimatti et al. 2004; Kitzbichler & White 2007; Cirasuolo et al. 2010). This study (and that of Henriques et al. 2010) suggest otherwise – current models seem fully capable of reproducing the data given realistic assessments of population synthesis uncertainties and of the effects of observational errors. A much more serious problem, as already pointed out by Guo et al. (2011), is that the models grow somewhat lower mass galaxies too early. Objects with $M_\star \sim 10^{10} M_\odot$ are already present

with a large fraction of their $z = 0$ abundance at redshifts of 2 or 3, whereas the observations indicate a drop in abundance by about an order of magnitude. Cosmic down-sizing thus appears much stronger in the real Universe than in the models. Reconciling theory and observation in the context of the ΛCDM cosmology will require star formation efficiencies to scale with mass and redshift in a very different way than current models (and simulations) assume.

ACKNOWLEDGEMENTS

REFERENCES

Baugh C. M., Lacey C. G., Frenk C. S., Granato G. L., Silva L., Bressan A., Benson A. J., Cole S., 2005, MNRAS, 356, 1191

Bell E. F., McIntosh D. H., Katz N., Weinberg M. D., 2003, ApJ Supp., 149, 289

Blaizot J., Wadadekar Y., Guiderdoni B., Colombi S. T., Bertin E., Bouchet F. R., Devriendt J. E. G., Hatton S., 2005, MNRAS, 360, 159

Bower R. G., Benson A. J., Malbon R., Helly J. C., Frenk C. S., Baugh C. M., Cole S., Lacey C. G., 2006, MNRAS, 370, 645

Bower R. G., Vernon I., Goldstein M., Benson A. J., Lacey C. G., Baugh C. M., Cole S., Frenk C. S., 2010, MNRAS, 407, 2017

Boylan-Kolchin M., Springel V., White S. D. M., Jenkins A., Lemson G., 2009, MNRAS, 398, 1150

Bruzual G., Charlot S., 2003, MNRAS, 344, 1000

Buzzoni A., 1989, ApJ Supp., 71, 817

Capak P., Aussel H., Ajiki M., et al., 2007, ApJ Supp., 172, 99

Capak P., Cowie L. L., Hu E. M., et al., 2004, AJ, 127, 180

Cattaneo A., Dekel A., Devriendt J., Guiderdoni B., Blaizot J., 2006, MNRAS, 370, 1651

Chabrier G., 2003, PASP, 115, 763

Charlot S., Bruzual G., 2007, in preparation, 1

Cimatti A., Daddi E., Renzini A., Cassata P., Vanzella E., Pozzetti L., Cristiani S., Fontana A., Rodighiero G., Mignoli M., Zamorani G., 2004, Nat., 430, 184

Cirasuolo M., McLure R. J., Dunlop J. S., Almaini O., Foucaud S., Simpson C., 2010, MNRAS, 401, 1166

Cole S., Aragon-Salamanca A., Frenk C. S., Navarro J. F., Zepf S. E., 1994, MNRAS, 271, 781

Cole S., Lacey C. G., Baugh C. M., Frenk C. S., 2000, MNRAS, 319, 168

Conroy C., Gunn J. E., White M., 2009, ApJ, 699, 486

Conroy C., White M., Gunn J. E., 2010, ApJ, 708, 58

Conselice C. J., Bundy K., U V., Eisenhardt P., Lotz J., Newman J., 2008, MNRAS, 383, 1366

Croton D. J., Springel V., White S. D. M., De Lucia G., Frenk C. S., Gao L., Jenkins A., Kauffmann G., Navarro J. F., Yoshida N., 2006, MNRAS, 365, 11

da Cunha E., Charlot S., Elbaz D., 2008, MNRAS, 388, 1595

Davis M., Faber S. M., Newman J., et al., 2003, in P. Guhathakurta ed., Proc. SPIE Vol. 4834 of Proc. SPIE, Science Objectives and Early Results of the DEEP2 Redshift Survey. pp 161–172

de la Torre S., Meneux B., De Lucia G., et al., 2011, Astronomy and Astrophysics Supplement Series, 525, A125+

De Lucia G., Blaizot J., 2007, MNRAS, 375, 2

Draine B. T., Dale D. A., Bendo G., et al., 2007, ApJ, 663, 866

Draine B. T., Li A., 2007, ApJ, 657, 810

Drory N., Bender R., Feulner G., Hopp U., Maraston C., Snigula J., Hill G. J., 2003, ApJ, 595, 698

Fazio G. G., Ashby M. L. N., Barmby P., et al., 2004, ApJ Supp., 154, 39

Fioc M., Rocca-Volmerange B., 1997, Astronomy and Astrophysics Supplement Series, 326, 950

Fontanot F., Monaco P., 2010, MNRAS, 405, 705

Fontanot F., Somerville R. S., Silva L., Monaco P., Skibba R., 2009, MNRAS, 392, 553

Gallazzi A., Bell E. F., 2009, ApJ Supp., 185, 253

Giallongo E., Salimbeni S., Menci N., Zamorani G., Fontana A., Dickinson M., Cristiani S., Pozzetti L., 2005, ApJ, 622, 116

Granato G. L., Lacey C. G., Silva L., Bressan A., Baugh C. M., Cole S., Frenk C. S., 2000, ApJ, 542, 710

Guo Q., White S., Boylan-Kolchin M., De Lucia G., Kauffmann G., Lemson G., Li C., Springel V., Weinmann S., 2011, MNRAS, 413, 101

Guo Q., White S. D. M., 2009, MNRAS, 396, 39

Henriques B., Maraston C., Monaco P., Fontanot F., Menci N., De Lucia G., Tonini C., 2010, ArXiv e-prints

Henriques B. M. B., Thomas P. A., 2010, MNRAS, 403, 768

Henriques B. M. B., Thomas P. A., Oliver S., Roseboom I., 2009, MNRAS, 396, 535

Ilbert O., Tresse L., Zucca E., et al., 2005, Astronomy and Astrophysics Supplement Series, 439, 863

Jones D. H., Peterson B. A., Colless M., Saunders W., 2006, MNRAS, 369, 25

Kampakoglou M., Trotta R., Silk J., 2008, MNRAS, 384, 1414

Kauffmann G., Colberg J., Diaferio A., White S., 1999, MNRAS, 303, 188

Kauffmann G., White S. D. M., Guiderdoni B., 1993, MNRAS, 264, 201

Keenan R. C., Barger A. J., Cowie L. L., Wang W.-H., 2010, ApJ, 723, 40

Kitzbichler M. G., White S. D. M., 2007, MNRAS, 376, 2

Lacey C. G., Baugh C. M., Frenk C. S., Benson A. J., Orsi A., Silva L., Granato G. L., Bressan A., 2010, MNRAS, 405, 2

Lawrence A., Warren S. J., Almaini O., et al., 2007, MNRAS, 379, 1599

Le Fèvre O., Vettolani G., Garilli B., et al., 2005, Astronomy and Astrophysics Supplement Series, 439, 845

Leitherer C., Schaerer D., Goldader J. D., González Delgado R. M., Robert C., Kune D. F., de Mello D. F., Devost D., Heckman T. M., 1999, ApJ Supp., 123, 3

Lemson G., Virgo Consortium t., 2006, ArXiv Astrophysics e-prints

Lu Y., Mo H. J., Weinberg M. D., Katz N. S., 2010, ArXiv e-prints

Maraston C., 1998, MNRAS, 300, 872

Maraston C., 2005, MNRAS, 362, 799

Marchesini D., van Dokkum P., Quadri R., et al., 2007, ApJ, 656, 42

Marigo P., Girardi L., 2007, Astronomy and Astrophysics Supplement Series, 469, 239

Mathis J. S., Mezger P. G., Panagia N., 1983, Astronomy and Astrophysics Supplement Series, 128, 212

McCarthy I. G., Frenk C. S., Font A. S., Lacey C. G., Bower R. G., Mitchell N. L., Balogh M. L., Theuns T., 2008, MNRAS, 383, 593

McCracken H. J., Radovich M., Bertin E., et al., 2003, Astronomy and Astrophysics Supplement Series, 410, 17

Menci N., Fontana A., Giallongo E., Grazian A., Salimbeni S., 2006, ApJ, 647, 753

Monaco P., Fontanot F., Taffoni G., 2007, MNRAS, 375, 1189

Norberg P., Cole S., Baugh C. M., et al., 2002, MNRAS, 336, 907

Poli F., Giallongo E., Fontana A., et al., 2003, ApJ, 593, L1

Pozzetti L., Cimatti A., Zamorani G., Daddi E., Menci N., Fontana A., Renzini A., Mignoli M., Poli F., Saracco P., Broadhurst T., Cristiani S., D'Odorico S., Giallongo E., Gilmozzi R., 2003, Astronomy and Astrophysics Supplement Series, 402, 837

Salimbeni S., Giallongo E., Menci N., et al., 2008, Astronomy and Astrophysics Supplement Series, 477, 763

Saracco P., Fiano A., Chincarini G., Vanzella E., Longhetti M., Cristiani S., Fontana A., Giallongo E., Nonino M., 2006, MNRAS, 367, 349

Saracco P., Giallongo E., Cristiani S., D'Odorico S., Fontana A., Iovino A., Poli F., Vanzella E., 2001, Astronomy and Astrophysics Supplement Series, 375, 1

Scoville N., Aussel H., Brusa M., et al., 2007, ApJ Supp., 172, 1

Somerville R. S., Gilmore R. C., Primack J. R., Dominguez A., 2011, ArXiv e-prints

Somerville R. S., Hopkins P. F., Cox T. J., Robertson B. E., Hernquist L., 2008, MNRAS, 391, 481

Somerville R. S., Primack J. R., 1999, MNRAS, 310, 1087

Spergel D. N., Verde L., Peiris H. V., et al., 2003, ApJ Supp., 148, 175

Springel V., White S. D. M., Jenkins A., et al., 2005, Nat., 435, 629

Springel V., White S. D. M., Tormen G., Kauffmann G., 2001, MNRAS, 328, 726

Thomas D., Maraston C., Bender R., 2003, MNRAS, 339, 897

Tonini C., Maraston C., Devriendt J., Thomas D., Silk J., 2009, MNRAS, 396, L36

Tonini C., Maraston C., Thomas D., Devriendt J., Silk J., 2010, MNRAS, 403, 1749

van der Wel A., Franx M., Wuyts S., van Dokkum P. G., Huang J., Rix H., Illingworth G. D., 2006, ApJ, 652, 97

Vazdekis A., Casuso E., Peletier R. F., Beckman J. E., 1996, ApJ Supp., 106, 307

Whitaker K. E., Labbe I., van Dokkum P. G., Brammer G., Kriek M., Marchesini D., Quadri R. F., Franx M., Muzzin A., Williams R. J., Bezanson R., Illingworth G. D., Lee K.-S., Lundgren B., Nelson E. J., Rudnick G., Tal T., Wake D. A., 2011, ArXiv e-prints

White S. D. M., Frenk C. S., 1991, ApJ, 379, 52

Willmer C. N. A., Faber S. M., Koo D. C., et al., 2006, ApJ, 647, 853

Worthey G., 1994, ApJ Supp., 95, 107

Wuyts S., Labbé I., Schreiber N. M. F., Franx M., Rudnick G., Brammer G. B., van Dokkum P. G., 2008, ApJ, 682, 985

Yasuda N., Fukugita M., Narayanan V. K., et al., 2001, AJ, 122, 1104

Zibetti S., Charlot S., Rix H.-W., 2009, MNRAS, 400, 1181

Zucca E., Bardelli S., Bolzonella M., ohters 2009, Astronomy and Astrophysics Supplement Series, 508, 1217